New Age Constraints on the Metamorphic Evolution of the High-Pressure/Low-Temperature Belt in the Western Tianshan Mountains, NW China

R. Klemd, M. Bröcker,[1] *B. R. Hacker,*[2] *J. Gao,*[3] *P. Gans,*[2] *and K. Wemmer*[4]

Mineralogisches Institut, Universität Würzburg, Am Hubland, 97074 Würzburg, Germany
(e-mail: reiner.klemd@mail.uni-wuerzburg.de)

ABSTRACT

The western Tianshan high-pressure/low-temperature orogenic belt in NW China contains eclogite-facies metavolcanic rocks and omphacite-bearing blueschists. Previous Sm-Nd (omphacite, garnet, glaucophane, whole rock) and $^{40}Ar/^{39}Ar$ (crossite) dating of eclogite-facies rocks has suggested an age of ca. 345 Ma as the best approximation for the timing of peak metamorphic conditions. The samples described here are blueschist-facies rocks that formed during or after the transition from the eclogite-facies to the epidote-blueschist-facies and subsequently experienced an incipient greenschist-facies overprint. By use of white mica geochronology (K-Ar, $^{40}Ar/^{39}Ar$, Rb-Sr), an attempt is made to date postpeak metamorphic stages of the complex *PT* path. Rb-Sr and $^{40}Ar/^{39}Ar$ ages range between 313 and 302 Ma and 323 and 312 Ma, respectively, but mostly cluster at ca. 310–311 Ma, indicating that the studied samples recrystallized at this time. However, the $^{40}Ar/^{39}Ar$ age spectra show complex release patterns that are interpreted to be influenced by excess argon to varying degrees. This conclusion is further corroborated by K-Ar dates ranging between 385 and 309 Ma. Younger dates of ca. 302 Ma (Rb-Sr) and ca. 296 Ma (K-Ar) indicate subsequent disturbances of these isotope systems in some rocks. The new ages are significantly younger than the time of eclogite-facies metamorphism (350–345 Ma), indicating resetting of the $^{40}Ar/^{39}Ar$, K-Ar, and Rb-Sr systems during exhumation of the blueschist-facies rocks. Furthermore, this dataset suggests that high-pressure conditions were attained during the Carboniferous and not at Permian or Triassic time, as recently suggested by SHRIMP U-Pb zircon dating.

Online enhancements: tables.

Introduction

The western Tianshan orogenic belt in NW China (fig. 1) formed within a Paleozoic accretionary wedge on the south side of the Yili–central Tianshan plate and contains several occurrences of high-pressure/low-temperature (HP-LT) rocks such as blueschists and eclogites (e.g., Gao et al. 1995, 1997, 1999). Reconstructing the *PTt*-d paths of these rocks is crucial for understanding the tectonometamorphic evolution of this orogen and developing plausible geodynamic models. Constructing such paths requires the determination of the prograde and retrograde *PT* evolution and the correlation of distinct metamorphic stages with geochronological data. Previous studies suggested that the eclogites and omphacite-bearing blueschists shared a common peak and postpeak metamorphic history. Peak metamorphic conditions were estimated at 480°–600°C and 14–21 kbar, based on conventional geothermobarometry and quantitative phase diagrams (Gao et al. 1999; Gao and Klemd 2000, 2001; Klemd et al. 2002; Wei et al. 2003). The possibility of ultrahigh pressure in some of those eclogites remains ambiguous (cf. Klemd 2003; Zhang et al. 2003*b*). Posteclogite-facies conditions between 9 and 14 kbar at 480°–570°C suggest a near-isothermal decompression path from eclogite- to epidote-amphibolite-facies conditions, similar to

Manuscript received March 23, 2004; accepted October 25, 2004.

[1] Institut für Mineralogie, Zentrallaboratorium für Geochronologie, Corrensstrasse 24, 48149 Münster, Germany.

[2] Department of Geological Sciences, University of California, Santa Barbara, California 93106-9630, U.S.A.

[3] Institute of Geology and Geophysics, Chinese Academy of Sciences, P.O. Box 9825, Beijing, China.

[4] Geowissenschaftliches Zentrum der Universität Göttingen, Goldschmidtstrasse 3, 37077 Göttingen, Germany.

[The Journal of Geology, 2005, volume 113, p. 157–168] 0022-1376/2005/11302-0003$15.00

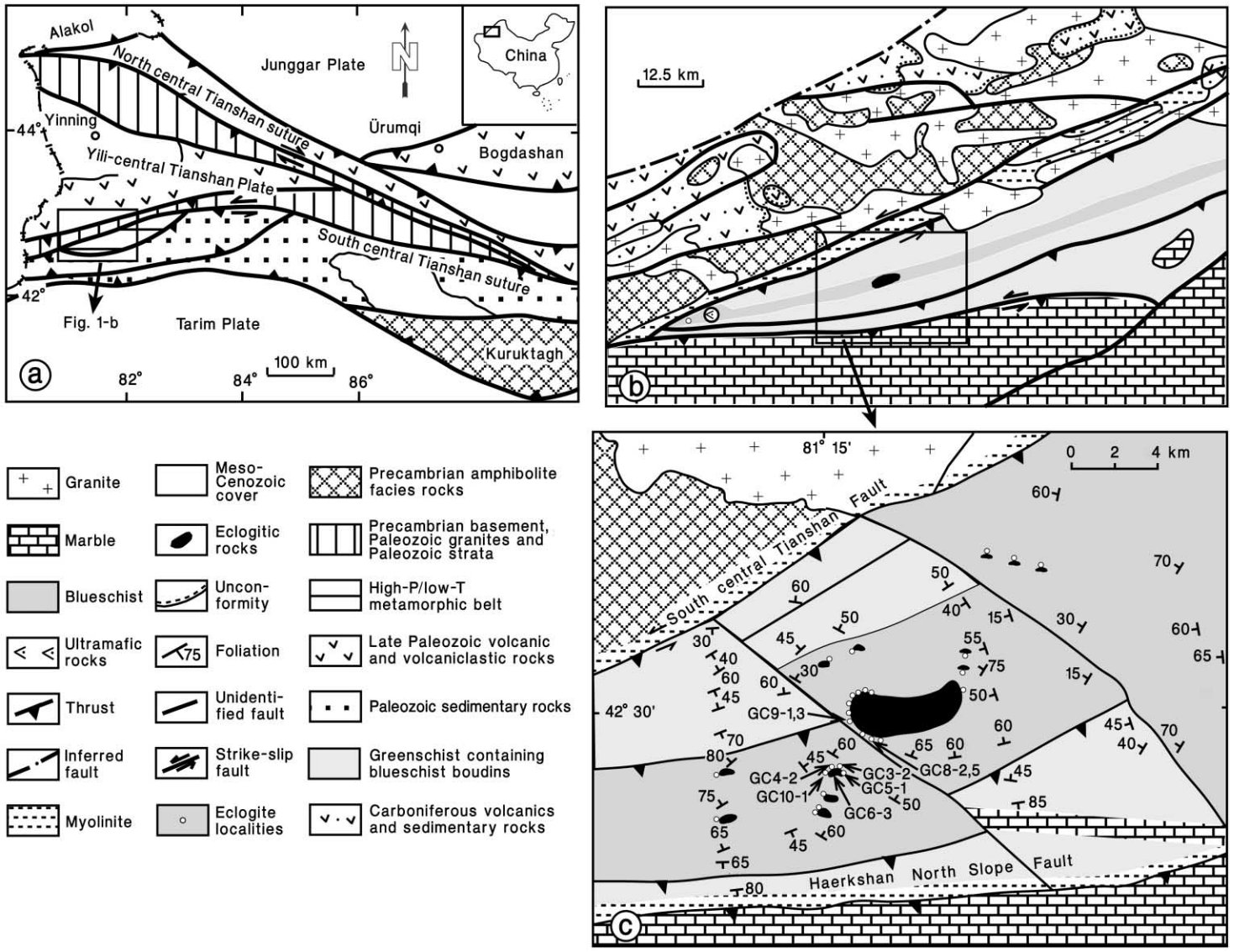

Figure 1. Geological map of the western Tianshan HP-LT metamorphic belt in northwestern China (modified after Gao et al. 1999). *a*, Regional geological map. *b*, Local geological map. *c*, Detailed geological map showing sample locations.

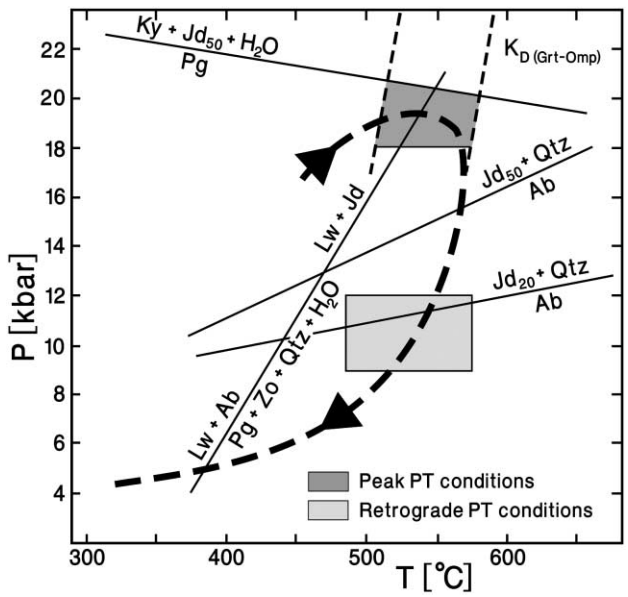

Figure 2. Metamorphic *PT* path of the western Tianshan HP-LT rocks (modified after Gao et al. 1999; Klemd et al. 2002).

that of an "alpine-type" tectonic setting (Klemd et al. 2002). Peak metamorphism is interpreted to have occurred at about 345 Ma, as suggested by Sm-Nd dating of a garnet-glaucophane pair from an eclogite, as well as by $^{40}Ar/^{39}Ar$ data for sodic amphibole from omphacite-bearing blueschists (Xiao et al. 1992; Gao et al. 1995; Gao and Klemd 2003). However, these geochronological results are in conflict with SHRIMP U-Pb zircon ages for HP rocks from the same area, interpreted to indicate that peak metamorphism is younger than 310 Ma (Zhang et al. 2002*a*). Further contributions suggested an age of ca. 215 Ma and a Permian age for the timing of eclogite-facies metamorphism (Zhang et al. 2002*b*, 2003*a*). To resolve the uncertainty caused by conflicting age information, we have studied blueschist-facies rocks, which represent a posteclogite-facies *PT* stage. K-Ar, $^{40}Ar/^{39}Ar$, and Rb-Sr dating of white mica provides further time constraints on the metamorphic evolution of the HP rocks in the western Tianshan.

Geological Setting

The Tianshan HP-LT belt extends for about 1500 km from NW China, across Kirghizia to Tajikistan, within the southern Tianshan Mountains (Sobolev et al. 1986; Gao et al. 1995, 1997; Tagiri et al. 1995; Volkova and Budanov 1999). This belt marks a subduction/collisional zone between the Yili-Kazakhstan-Kyzylkum and the Tarim-Karakum plates (Volkova and Budanov 1999). In the Chinese Tianshan, the HP-LT belt extends along the south central Tianshan suture for at least 200 km, separating the Tarim plate to the south and the Yili–central Tianshan plate to the north (fig. 1*a*).

A Paleozoic active continental margin is exposed north of the HP-LT belt (Gao et al. 1998). It is composed mainly of Precambrian amphibolite-facies schists, granulites, gneisses and metabasic rocks, Late Silurian and Early Carboniferous island-arc type volcanics and volcaniclastic rocks, as well as Caledonian-Variscan granitoids. The HP-LT belt is separated from the active margin by a broad ductile shear zone that consists of a 7.5-km-wide zone of thrust sheets transported toward the north-northwest at the end of the Early Carboniferous and a 0.5-km-wide sinistral strike-slip shear zone (Gao et al. 1997). The HP-LT belt is overlain by a succession of unmetamorphosed Paleozoic sediments interpreted as the passive continental margin of the Tarim plate (Allen et al. 1993; Carroll et al. 1995).

The HP-LT sequences comprise mafic metavolcanic rocks, metavolcaniclastic rocks, metagreywacke, marble, and slices of ultramafic rocks, and they possibly represent a mélange formed within an accretionary wedge on the south side of the Yili–central Tianshan plate (Gao et al. 1999). The metavolcanic rocks include eclogite, omphacitite, epidosite, and blueschist (e.g., Klemd et al. 2002). Garnet, omphacite, zoisite, epidote minerals, phengite, paragonite, sodic amphibole, quartz, titanite, and rutile are present in all mafic rocks in variable modal proportions. Eclogites and omphacitites occur as pods (15–25 cm in diameter), boudins (0.2×0.5 to 5×20 m^2), thin layers (2–50 cm in thickness), or large massive blocks (almost 2 km^2 in plan view) within blueschist layers. Blueschists occur as coherent layers of variable thickness and as discrete blocks and lenses in greenschist-facies metasedimentary rocks (fig. 1*b*, 1*c*). Two types of blueschist are recognized: the first type lacks a foliation and may contain omphacite; albite is rare or absent. Individual layers of eclogite have tectonically undisturbed contacts with intimately interlayered omphacite-bearing blueschist, and previous studies suggested that both rock types experienced identical peak metamorphic conditions (e.g., Gao et al. 1999; Klemd et al. 2002). The second blueschist type generally is much more retrogressed and displays a well-defined foliation. These rocks are albite bearing; omphacite is rare or absent. The foliation of the retrograde blueschist is predominantly parallel to that of the enclosing metasedimentary greenschists and belongs to the main ENE

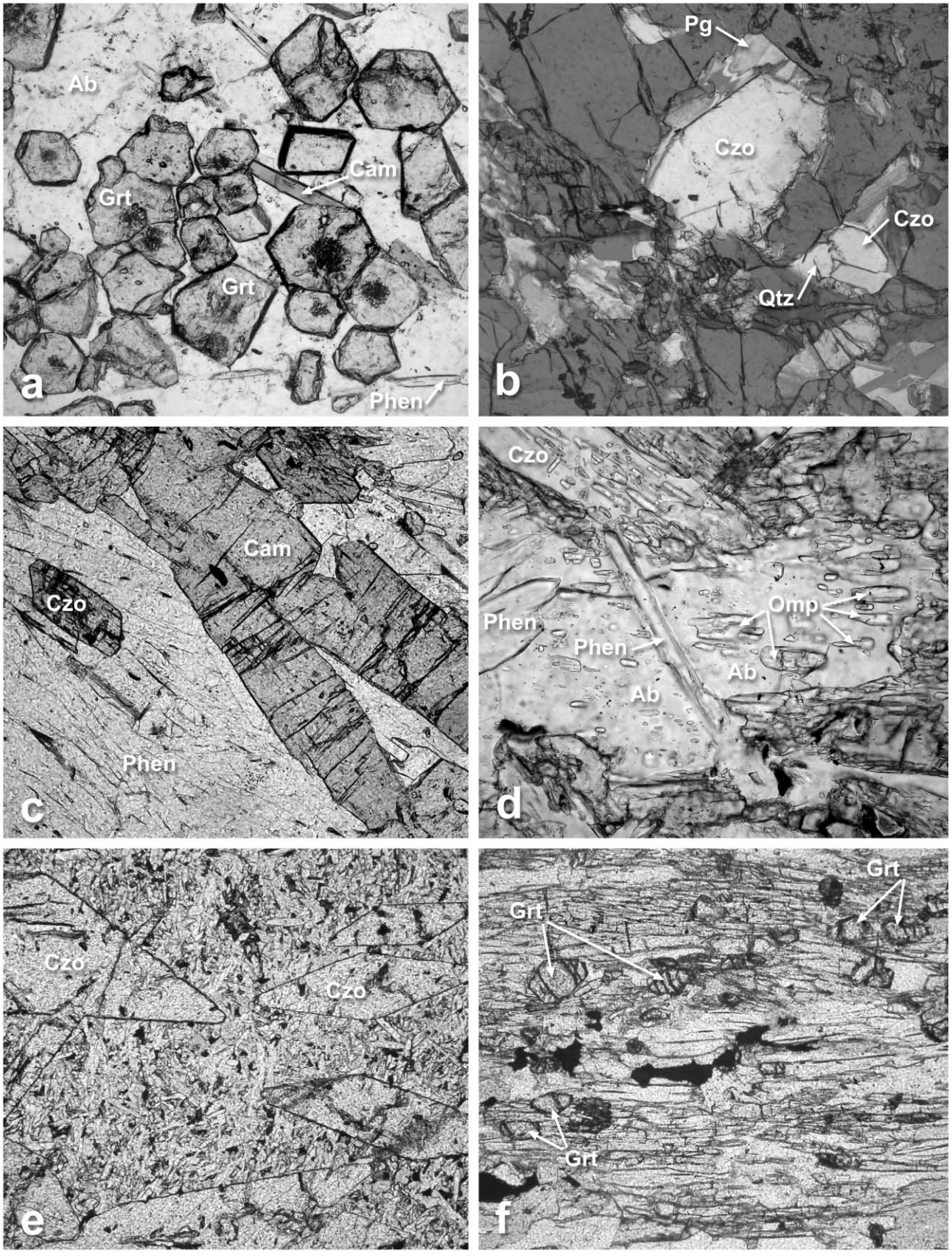
Ab
Cam
Grt
Grt
Phen
a
Pg
Czo
Czo
Qtz
b
Cam
Czo
Phen
c
Czo
Phen
Phen
Omp
Ab
Ab
d
Czo
Czo
e
Grt
Grt
Grt
f

regional trend. Some eclogite-facies veins occur in massive omphacite-bearing blueschists and eclogites, indicating that a free fluid phase was present under peak eclogite-facies conditions (Gao and Klemd 2001). In fact, the largest eclogite block (fig. 1*c*) is composed not only of true eclogite (garnet ± omphacite > 70%; Carswell 1990) but also of omphacitite, epidosite, and omphacite-bearing blueschist that are cut by eclogite-facies veins. Trace element characteristics (including REE) of the metabasic rocks suggest MORB to oceanic island basalt affinities interpreted to indicate a seamount-like setting for the protolith (Gao and Klemd 2003).

Previous Geochronology

Xiao et al. (1992) and Gao et al. (1995) reported $^{40}Ar/^{39}Ar$ plateau ages of 350.9 ± 2 Ma and 345.5 ± 7 Ma for glaucophane and phengite, respectively, for blueschist from the western Tianshan. Similar results were obtained by use of the Sm-Nd method for an eclogite from the same area (Gao and Klemd 2003). This eclogite yielded an errorchron age of 343 ± 44 Ma (omphacite, garnet, glaucophane, whole rock). The Sm-Nd garnet-glaucophane age of 346 ± 3 Ma is concordant with the $^{40}Ar/^{39}Ar$ results for crossite from the same exposure, indicating an age of 344 ± 3 Ma. Consequently, an age of ca. 345 Ma has been suggested as the best approximation for the timing of eclogite-facies *PT* conditions (for discussion see Gao and Klemd 2003). In addition, Gao and Klemd (2003) reported an $^{40}Ar/^{39}Ar$ plateau age of 331 ± 2 Ma for phengite, which was interpreted to represent the stage in which the HP-LT rocks have been exhumed to higher tectonic levels.

Older $^{40}Ar/^{39}Ar$ ages for HP rocks of the western Tianshan (ca. 401 and 364 Ma, sodic amphibole, phengite) were reported by Gao et al. (2000), while Zhang et al. (2003*a*, 2002*b*) postulated a significantly younger age for the eclogite-facies metamorphism in the same area (<310 and 215 Ma), based on "preliminary" SHRIMP U-Pb analyses of zircon.

Further, it should also be noted that eclogites from the southern Tianshan of Kirghistan provided possible indications for three different eclogite-facies events at 749 ± 14 Ma (Omp-Hbl-Rt-WR, Rb-Sr isochron), 482 ± 5 Ma (K-Ar cooling ages from paragonite), and 267 ± 5 Ma (Omp-Grt-PhI-PhII-WR, Rb-Sr isochron) (Tagiri et al. 1995).

Petrology and Sample Description

The prograde metamorphic evolution of the eclogites and omphacite-bearing blueschists of the western Tianshan has been extensively discussed by Gao et al. (1999), Gao and Klemd (2000), Klemd et al. (2002), and Wei et al. (2003). These authors demonstrated the prograde transition from lawsonite-blueschist/epidote-blueschist facies to eclogite-facies conditions at 500°–600°C and 14–21 kbar (fig. 2). The maximum pressure mineral paragenesis consists of garnet-omphacite-quartz-glaucophane-phengite/paragonite and minor carbonate, rutile, and apatite. Decompression caused the destabilization of omphacite, garnet, and glaucophane to albite, Ca-amphibole, and chlorite. The posteclogite-facies conditions between 9 and 14 kbar at 480°–570°C suggest an almost isothermal decompression from eclogite to epidote-amphibolite-facies conditions, which was followed by simultaneous cooling and decompression to greenschist-facies conditions (fig. 2) (Gao et al. 1999; Klemd et al. 2002). Here, we describe posteclogite-facies mineral assemblages (fig. 3), following the peak assemblages as described above. Apart from inclusions in garnet and albite (fig. 3*d*), omphacite was only recognized as a relict in the matrix of samples GC 4-2, GC 8-2, GC 8-5, and GC 9-1. Five samples (GC 6-3, GC 8-2, GC 8-5, GC 9-1, GC 9-3) contain the mineral assemblage garnet-phengite-paragonite-glaucophane-clinozoisite-rutile (table 1). Glaucophane occurs either as a matrix mineral (fig. 3*e*, 3*f*) or as a porphyroblast with inclusions of clinozois-

Figure 3. Photomicrographs showing the textural relationship and paragenesis of the HP-LT rocks of the western Tianshan. *a*, Idioblastic garnets surrounded by coarse-grained albite (sample GC 4-2; plane light, width of view = 4 mm). *b*, Box-shaped clinozoisite-paragonite-quartz intergrowth (after lawsonite?) in garnet (sample GC 9-3; crossed nicols, width of view 0.5 mm). *c*, Porphyroblastic winchite in foliated phengite matrix (sample GC 9-1; plane light, width of view = 4 mm). *d*, Albite porphyroblast with omphacite and phengite inclusions (sample GC 4-2; plane light, width of view = 2 mm). *e*, Porphyroblastic clinozoisite in a matrix of fine-grained glaucophane (sample GC 8-5; plane light, width of view = 4 mm). *f*, Fine-grained garnets in foliated blueschist. The foliation is defined by glaucophane, phengite, and opaque minerals (sample GC 10-1; plane light, width of view = 4 mm). Mineral abbreviations are after Kretz (1983).

Table 1. Mineral Assemblages (vol%) of the Analyzed High-Pressure Rocks from the Study Area

Sample	Grt	Omp	Gln	Pg/Phen	Qtz	Ab	Zo/Czo	Chl	Carb	Rt	Ttn	Hrbl	Opaque
GC 3-2	5	−	5	15	15	50	−	3	5	−	−	+	2
GC 4-2	16	4R	+	19[a]	20	24	5	+	+	−	2	7	3
GC 5-1	15	−	5	7[b]	20	45	+	1	2	−	2	+	3
GC 6-3	5	−	25	20[a]	20	18	+	2	5	+	2	−	3
GC 8-2	5	+	68	5[b]	2	+	10	2	3	+	−	+	5
GC 8.5	5	+	62	5	5	−	20	−	+	+	1	−	2
GC 9-1	10	+	37	30[b]	5	−	+	+	−	+	1	15	2
GC 9-3	30	−	35	10[b]	10	−	+	2	8	1	−	2	2
GC 10-1	10	−	22	20[a]	20	+	+	5	20	+	1	+	3

Note. Omp = omphacite inclusions in garnet or albite, or as relic (R). Opaque = ilmenite, pyrite, and magnetite. Plus sign = present; minus sign = not observed.
[a] Only paragonite (rare phengite mainly as inclusion in garnet or albite).
[b] Only phengite (rare paragonite inclusions in garnet).

ite, omphacite, phengite, paragonite, and magnetite. Most garnet porphyroblasts contain clinozoisite, paragonite, and omphacite inclusions (fig. 3*b*), indicating that the rocks are retrogressed omphacite-bearing blueschists or eclogites. Paragonite and phengite occur as large flakes (0.5–2 mm) intimately intergrown in the matrix (fig. 3*a*, 3*d*, 3*f*). A moderate greenschist-facies overprint is displayed by albite, chlorite, calcic-amphibole, and carbonate, which occur along rims and fractures of primary minerals. The other four more retrogressed samples (GC 3-2, GC 4-2, GC 5-1, GC 10-1) show a well-pronounced foliation defined by coarse-grained phengite, paragonite, and, in places, glaucophane (fig. 3*f*). Glaucophane and garnet are commonly replaced either by albite, winchite, and actinolite or by garnet and quartz, respectively (fig. 3*a*, 3*c*, 3*d*). Secondary chlorite, quartz, and carbonate are ubiquitous, and rutile has been replaced by titanite (for a more detailed description of the different rock types, see Gao et al. 1999 and Klemd et al. 2002).

Analytical Methods

The compositions of phengite and paragonite were determined with an SX-50 CAMECA electron microprobe at the Mineralogisches Institut, Universität Würzburg (for further details, see Gao and Klemd 2001). Representative electron microprobe analyses of phengite and paragonite are shown in tables A1 and A2 in the online edition of the *Journal of Geology* (also available from the *Journal of Geology*'s Data Depository, free of charge upon request).

White mica separates were prepared by crushing hand samples, sieving, and cleaning in an ultrasonic bath with deionized water. White mica was concentrated from the 200–300-μm sieve fraction and was further purified by hand picking.

Nine samples were studied using the K-Ar dating method at the Geowissenschaftliches Zentrum, Universität Göttingen. The analytical error for the K/Ar age calculations is given on a 95% confidence level (2σ). Details of argon and potassium analyses for the laboratory in Göttingen are given in Wemmer (1991). K-Ar data of the studied samples is shown in table 2.

Rb-Sr analyses were carried out at the Zentrallaboratorium für Geochronologie at the Institut für Mineralogie, Universität Münster. Analytical details are reported in Bröcker et al. (2004). Rb-Sr isotope results are shown in table 3.

Six samples were investigated with the $^{40}Ar/^{39}Ar$ technique at the Geological Sciences Department, University of California, Santa Barbara, using techniques described by Calvert et al. (1999). $^{40}Ar/^{39}Ar$ analytical data are summarized in tables B1–B5 in the online edition of the *Journal of Geology* (also available from the *Journal of Geology*'s Data Depository, free of charge upon request).

Table 2. Analytical Data of K-Ar Age Determinations on Phengite and Paragonite

Sample	K_2O (wt%)	$^{40}Ar^*$ (nL/g) STP	$^{40}Ar^*$ (%)	Age (Ma)	2σ-error (%)
GC 3-2	7.70	84.48	76.98	311.7	9.7
GC 4-2	1.50	15.58	80.44	296.3	16.3
GC 5-1	9.91	114.63	94.11	327.1	9.1
GC 6-3	.83	11.49	74.43	385.1	13.1
GC 8-2	10.34	118.31	96.74	323.9	7.4
GC 8-5	5.99	65.13	96.11	309.1	8.6
GC 9-1	10.71	123.16	95.84	325.4	7.7
GC 9-3	10.61	121.04	97.87	323.0	6.6
GC 10-1	.74	8.52	78.54	325.7	11.5

Table 3. Rb-Sr Isotope Data for Blueschist-Facies Rocks from the Western Tianshan

Sample/mineral	Rb (ppm)	Sr (ppm)	$^{87}Rb/^{86}Sr$	$^{87}Sr/^{86}Sr$ ($\pm 2\sigma$)	Age (Ma) $\pm 2\sigma$
GC 3-2:					
White mica	165	255	1.87	.715846 (16)	313.0 ± 3.8
Whole rock	24.6	236	.303	.708870 (17)	
GC 5-1:					
White mica	193	106	5.26	.729147 (15)	301.6 ± 3.4
Whole rock	18.7	92.8	.584	.709065 (13)	
GC 8-2:					
White mica	215	60.7	10.3	.751900 (13)	309.4 ± 2.3
Epidote	2.44	2168	.00325	.706608 (16)	
Glaucophane	2.40	8.39	.829	.710246 (13)	
GC 8-5:					
White mica	121	77.9	4.49	.726696 (19)	309.0 ± 3.0
Epidote	.58	1208	.00138	.706949 (13)	
GC 9-1:					
White mica	243	24.0	29.6	.838148 (16)	310.7 ± 3.2
Whole rock	51.8	101	1.48	.713626 (13)	
GC 9-3:					
White mica	250	23.8	30.8	.843267 (63)	310.1 ± 3.1
Whole rock	21.7	57.4	1.09	.712225 (17)	
Whole rock	22.1	59.3	1.08	.712141 (17)	

Note. Based on repeated measurements, the $^{87}Rb/^{86}Sr$ ratios were assigned an uncertainty of 1%. Numbers in parentheses indicate within-run uncertainty on the last digits. In the course of this study, repeated runs of NBS standard 987 gave an average $^{87}Sr/^{86}Sr$ ratio of 0.710278 ± 0.000024 (2σ, $n = 17$). Total procedural blanks were less than 0.1 ng for Rb and 0.24 ng for Sr.

Results

White Mica Composition. White mica composition of all samples selected for geochronological studies were analyzed with the electron microprobe. Forty to 50 spot analyses were made for each sample, indicating that white mica is paragonite and/or phengite (tables A1, A2). Phengite shows a wide range in composition with regard to the Si content per formula unit (p.f.u.) and the X_{Fe} [Fe/(Fe + Mg)] content. Matrix phengite and phengite in contact with garnet in less retrogressed samples without additional paragonite (GC 8-2, GC 9-1, GC 9-3) have Si values ranging from 6.52 to 7.39 p.f.u. (on the basis of 22 oxygen) and X_{Fe} between 0.19 and 0.47. The phengite in contact with garnet usually has a higher X_{Fe} than the matrix phengite, indicating retrograde Fe-Mg exchange between garnet and phengite. Both matrix phengite and phengite in contact with garnet, which coexist with paragonite (GC 6-3, GC 8-5), show somewhat lower Si values of 6.55–6.73 p.f.u. when compared to phengite without coexisting paragonite. This indicates that the celadonite substitution depends on the presence of an additional aluminous phase such as paragonite. X_{Fe} in these less retrogressed samples ranges between 0.26 and 0.45. Phengite inclusions in garnet show an identical chemical composition when compared to matrix phengite. The electron microprobe analyses reveal significant chemical differences within single grains.

Matrix phengite and phengite in contact with garnet in the strongly retrogressed samples with or without paragonite (GC 3-2, GC 5-1, GC 10-1) have Si values between 6.62 and 6.95 p.f.u. and an X_{Fe} of 0.27 and 0.40; the composition of phengite inclusions in garnet is similar. As is the case in the less overprinted samples, high Si correlates with low X_{Fe}. Where present, matrix paragonite generally is close to endmember composition with a strong variation in X_{Fe} (0.35–0.76). Low Si contents correlate with high X_{Fe}, as was already shown for phengite. Some paragonite inclusions in garnet (GC 6-3) are characterized by very low X_{Fe} (<0.1), indicating that these inclusions formed during prograde *PT* conditions.

K-Ar Dating. The ages of white mica from the four mainly phengite-bearing samples (GC 5-1, GC 8-2; GC 9-1, and GC 9-3) are 327 ± 9 Ma, 324 ± 7 Ma, 325 ± 8 Ma, and 323 ± 7 Ma, respectively (table 2). Three white mica concentrates from the mainly paragonite-bearing samples (GC 4-2, GC 6-3, and GC 10-1) were dated at 296 ± 16 Ma, 385 ± 13 Ma, and 326 ± 12 Ma, respectively. The mixed paragonite and phengite samples GC 3-2 and GC 8-5 indicate ages of 312 ± 10 Ma and 309 ± 9 Ma.

Rb-Sr Dating. For Rb-Sr studies, six samples were selected. For four samples, age calculations are based on phengite–whole rock pairs (fig. 4; table 3). For two other samples, ages are based on

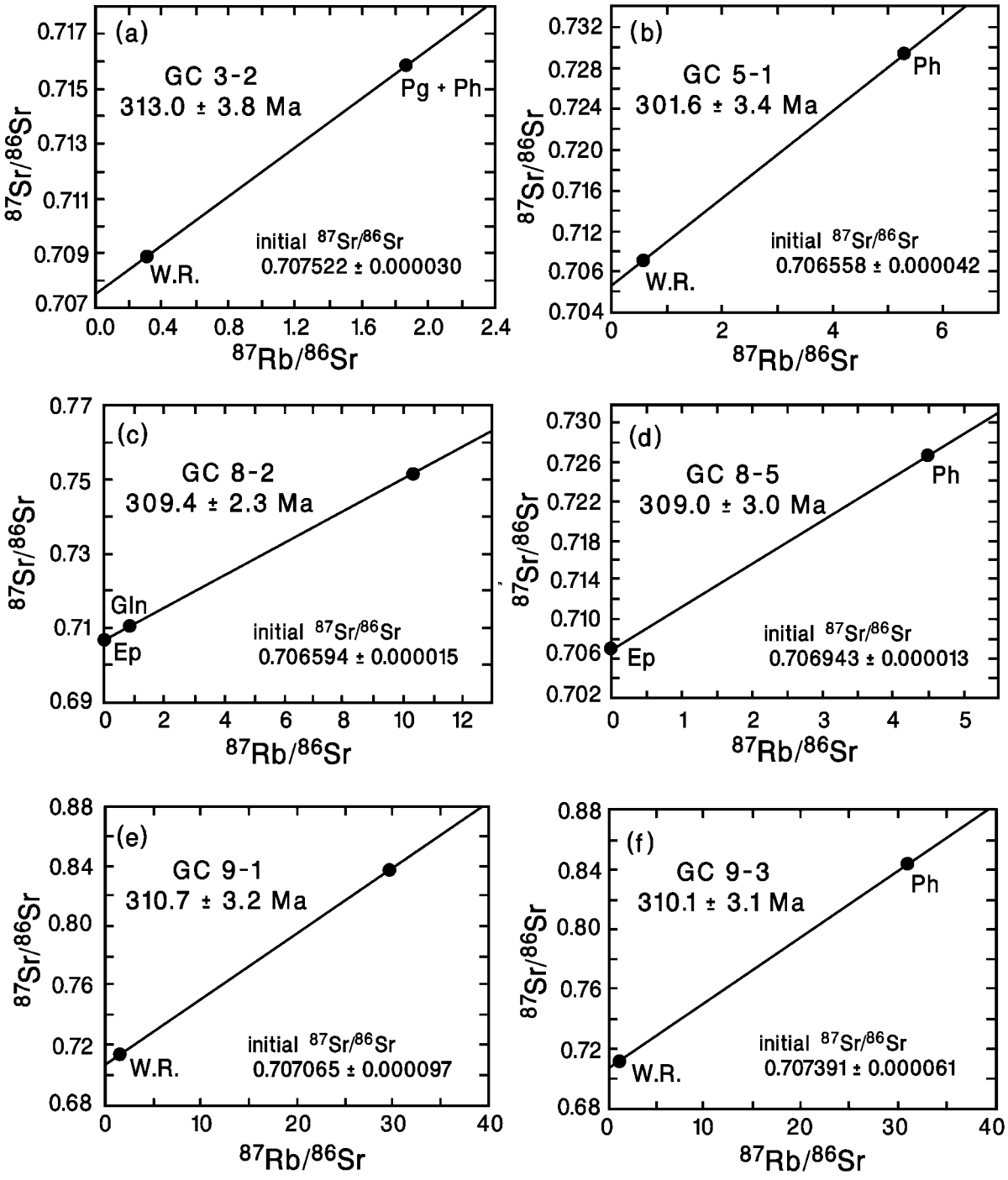

Figure 4. Rb-Sr isochrones for whita mica of blueschist-facies rocks from the western Tianshan

phengite-glaucophane and/or epidote. Four samples (GC 5-1, GC 8-2, GC 9-1, GC 9-3) almost exclusively contain phengite with ages of 301.6 ± 3.4 Ma, 309.4 ± 2.3 Ma, 310.7 ± 3.2 Ma, and 310.1 ± 3.1 Ma. Samples GC 3-2 and GC 8-5, containing more paragonite than phengite, display ages of 313.0 ± 3.8 Ma and 309 ± 3 Ma, respectively.

$^{40}Ar/^{39}Ar$ Dating. $^{40}Ar/^{39}Ar$ analytical results were obtained for the phengite-rich concentrates (four samples) and for one paragonite-rich concentrate (tables B1–B5). The spectrum for phengite sample GC 8-2 (fig. 5*a*) yields a well-defined plateau of 311.6 ± 0.9 Ma (2σ), which comprises six steps and about 62% of the ^{39}Ar released. Sample GC 5-

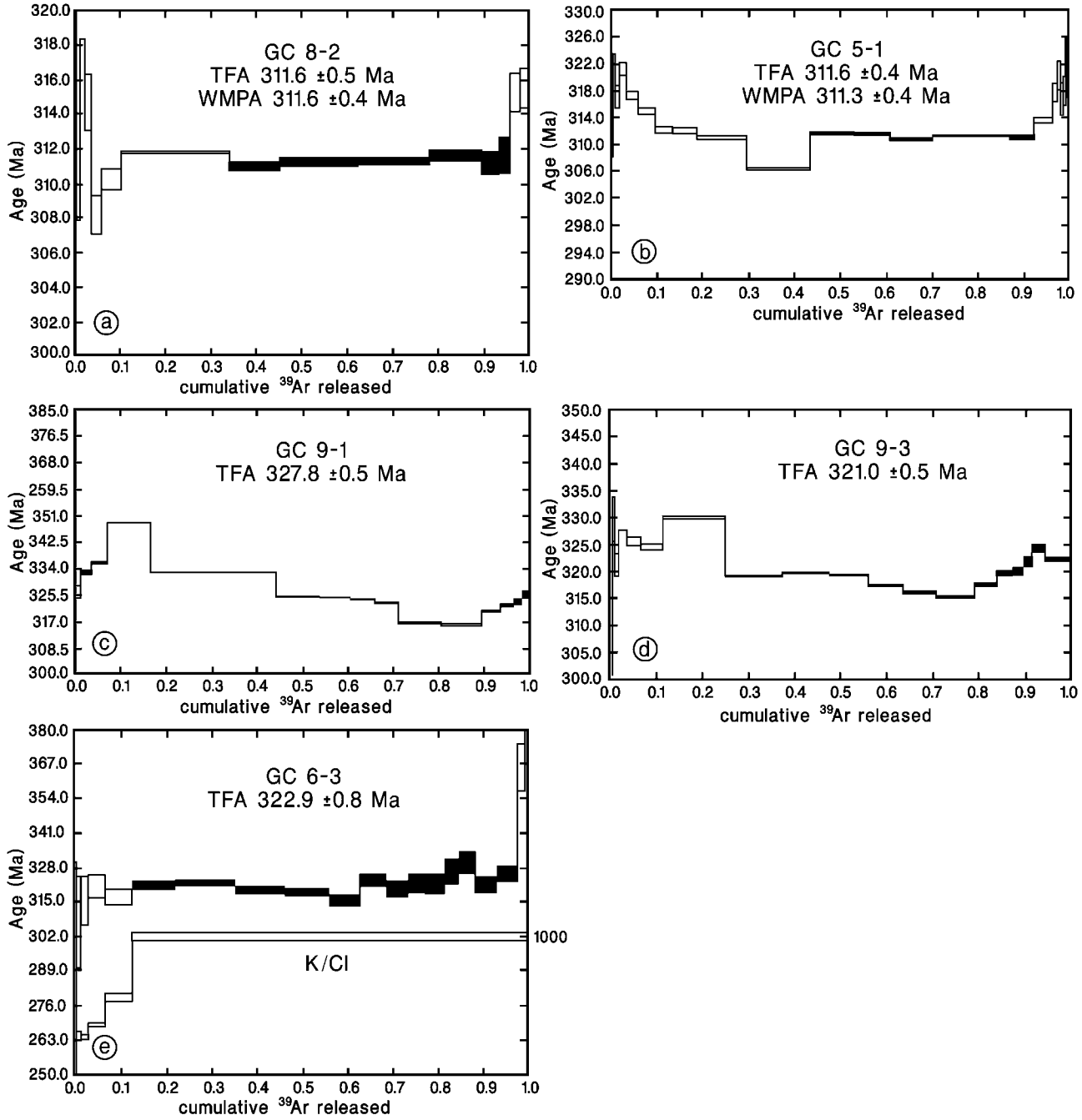

Figure 5. Ar age spectra for whita mica of blueschist-facies rocks from the western Tianshan. *TFA* = total fusion age; *WMPA* = weighted mean plateau age.

1 shows a more pronounced saddle-shaped spectrum (fig. 5*b*) and a less well developed plateau age of 311.3 ± 0.9 Ma, comprising five steps and about 50% of the ^{39}Ar release, and a total fusion age of 311.6 ± 0.9 Ma. The ^{40}Ar/^{39}Ar age spectra of the other two phengite concentrates (GC 9-1 and GC 9-3) are significantly more disturbed (figs. 5*c*, 5*d*). An isochron fit to isotopic ratios that make up 70% of the ^{39}Ar from GC 9-1 gives an age of 311.2 ± 5.0 Ma (MSWD = 1.93). There are no isochron fits for GC 9-3. The ^{40}Ar/^{39}Ar spectrum of paragonite GC 6-3 (fig. 5*e*) is nearly flat but does not form a plateau; removing the first five steps that have low K/Cl ratios and the last two steps that are not iso-

chronous with the remaining steps yields an inverse isochron of 310.9 ± 18.0 Ma with a $^{40}Ar/^{36}Ar$ ratio of 356 ± 27.

Discussion and Conclusions

The five $^{40}Ar/^{39}Ar$ white mica age spectra (fig. 5; see table C1 in the online edition of the *Journal of Geology* [also available from the *Journal of Geology*'s Data Depository, free of charge upon request]) are variably disturbed, with the phengites in particular showing (1) saddle shapes typical of samples containing excess ^{40}Ar or (2) $^{40}Ar/^{39}Ar$ ratios significantly greater than atmosphere (cf. Harrison and McDougall 1980). Three of the $^{40}Ar/^{39}Ar$ spectra (GC 9-1, GC 9-3, GC 6-3) have total fusion ages of 321–328 Ma, within error of the K/Ar ages (table C1), indicating that the K/Ar and $^{40}Ar/^{39}Ar$ age determinations are in agreement. These two observations imply that the differences between the K/Ar ages and the plateau or isochron ages for the samples GC 5-1 and GC 8-2 include excess ^{40}Ar that was perhaps removed during early in vacuo heating of the $^{40}Ar/^{39}Ar$ samples. Excess Ar is also considered to be the most plausible explanation for the $^{40}Ar/^{39}Ar$ dates (ca. 401 and 364 Ma) reported by Gao et al. (2000), who sampled the same outcrop area. Whether the excess Ar was derived from external fluids or inherited from the rock itself (Scaillet 1998; Sherlock and Arnaud 1999; Sherlock and Kelley 2002) cannot be evaluated from our data.

Two factors raise the possibility that all the $^{40}Ar/^{39}Ar$ ages—even those with plateaus—are affected by excess Ar (Sherlock and Arnaud 1999): (1) the clear demonstration of excess Ar in some of the samples and (2) the coincidence between the Rb/Sr and $^{40}Ar/^{39}Ar$ ages, for which white mica closure temperatures differ by 100°C or more (Hodges 1991). Point (2) is diffused somewhat by the fact that all the plateau and isochron ages are the same; if the ages were influenced by excess Ar that we cannot identify with isochron analysis, they might be expected to be different because of variable external Ar influx or variable bulk-rock K content. Point (2) can be explained without calling upon excess Ar if the Rb/Sr and $^{40}Ar/^{39}Ar$ systems yield the same ages because of either rapid cooling or recrystallization at temperatures close to or below the Rb/Sr closure.

It seems reasonable to suggest that resetting of the $^{40}Ar/^{39}Ar$ and Rb-Sr systems as well as the wide spectrum of white mica composition was caused by deformation-enhanced recrystallization under epidote-blueschist-facies *PT* conditions during hydration of the "anhydrous" eclogite assemblages. Besides the influence of excess Ar, the following alternatives may have been of importance for the complexity of our geochronological dataset. First, hydration of eclogites and the corresponding transformation into retrograde blueschists is strongly controlled by local availability of fluids and the presence or development of suitable infiltration paths; nonpervasive and variable fluid influx may have affected different rock volumes at different times. Second, the range in ages may suggest different episodes of exhumation and juxtaposition of tectonic slabs at higher crustal levels, although no structural or geological evidence for tectonic stacking was recognized. Third, the Rb-Sr and the $^{40}Ar/^{39}Ar$ systems in white mica have experienced disturbance and variable degrees of incomplete resetting during the eclogite-blueschist transition and/or the late greenschist-facies overprint. Furthermore, and finally, some samples represent mixtures of phengite and paragonite, which may represent different metamorphic stages, or may show different behavior during overprinting. At this point of our study we cannot unambiguously demonstrate which of these alternatives has influenced the white mica ages of the blueschist-facies rocks and a precise age for this *PT* stage cannot be given.

The general pattern for timing of metamorphism emerging from our dataset clearly suggests that the age of HP metamorphism is Carboniferous and not Permian or Triassic as postulated by Zhang et al. (2003*a*, 2002*b*) on the basis of preliminary unpublished SHRIMP data. Our Rb-Sr results indicate that the studied samples underwent a major episode of cooling or recrystallization around 311–310 Ma, with four out of six samples yielding ages around 310 Ma (fig. 4). The $^{40}Ar/^{39}Ar$ ages, which cluster around ~311 Ma (fig. 5), support this interpretation—although they may be affected by unresolved excess Ar. K-Ar dating (table 2) fits into the broad picture, but interpretation of this data is hampered by the much higher analytical uncertainty (2%–3%) and contamination by excess Ar. The significance of the discrepancy between K-Ar and $^{40}Ar/^{39}Ar$ ages of sample 6-3 (385 and 321 Ma) is unknown but may indicate sample inhomogeneity rather than excess ^{40}Ar. In accord with their postpeak high-pressure mineral assemblages, the samples studied here are significantly younger (ca. 35 Ma) than the age proposed for the eclogite-facies stage (ca. 350-345 Ma; Xiao et al. 1992; Gao et al. 1995; Gao and Klemd 2003), indicating that subsequent overprinting during exhumation has influenced the isotopic systems used for white mica geochronology.

ACKNOWLEDGMENTS

This study was funded by the State Key Project for Basic Research of China (2001 CB409803), the Funds for Hundred Outstanding Talents Plan sponsored by the Chinese Academy of Sciences, the National Natural Science Foundation of China (grants 49972079 and 49632240), the Deutsche Forschungsgemeinschaft (grant KL 692/10-2), and the U.S. National Science Foundation (grant EAR-0003568). We would like to thank members of the National 305 project and Xinjiang Bureau of Geological and Mineral Resources for their support in the field. We also thank D. A. Carswell, S. C. Sherlock, and an anonymous reviewer for helpful comments.

REFERENCES CITED

Allen, M. B.; Windley, B. F.; and Zhang, C. 1993. Paleozoic collisional tectonics and magmatism of the Chinese Tien Shan, central Asia. Tectonophysics 220:89–115.

Bröcker, M.; Bieling, D.; Hacker, B.; and Gans, P. 2004. High-Si phengite records the time of greenschist facies overprinting: implications for models suggesting mega-detachments in the Aegean Sea. J. Metamorph. Geol. 22:427–442.

Calvert, A. T.; Gans, P. B.; and Amato, J. M. 1999. Diapiric ascent and cooling of a sillimanite gneiss dome revealed by $^{40}Ar/^{39}Ar$ thermochronology: the Kigluaik Mountains, Seward Peninsula, Alaska. *In* Ring, U.; Brandon, M. T.; Lister, G.; Willett, S., eds. Exhumation processes: normal faulting, ductile flow, and erosion. London, Geological Society of London, p. 205–232.

Carroll, A. R.; Graham, S. A.; Hendrix, M. S.; Ying, D.; and Zhou, D. 1995. Late Paleozoic tectonic amalgamation of northwestern China: sedimentary record of the northern Tarim, northwestern Turpan, and southern Junggar Basin. Geol. Soc. Am. Bull. 107:571–594.

Carswell, D. A. 1990. Eclogite facies rocks. Glasgow and London, Blackie, 396 p.

Gao, J.; He, Q.; and Li, M. 1997. Studies on the features of the structural deformations on the West Tianshan orogenic belt. Acta Geosci. Sin. 18:1–10.

Gao, J.; He, G.; Li, M.; Tang, Y.; Xiao, X.; Zhou, M.; and Wang, J. 1995. The mineralogy, petrology, metamorphic PTDt trajectory and exhumation mechanism of blueschists, south Tianshan, northwestern China. Tectonophysics 250:151–168.

Gao, J., and Klemd, R. 2000. Eclogite occurrences in the western Tianshan high-pressure belt, Xinjiang, western China. Gondwana Res. 3:33–38.

———. 2001. Primary fluids entrapped at blueschist to eclogite transition: evidence from the Tianshan metasubduction complexes in northwestern China. Contrib. Mineral. Petrol. 142:1–14.

———. 2003. Formation of HP-LT rocks and their tectonic implications in the western Tianshan Orogen, NW China: geochemical and age constraints. Lithos 66:1–22.

Gao, J.; Klemd, R.; Zhang, L.; Wang, Z.; and Xiao, X. 1999. P-T path of high pressure-low temperature rocks and tectonic implications in the western Tianshan Mountains (NW China). J. Metamorph. Geol. 17:621–636.

Gao, J.; Li, M.; He, G.; Xiao, X.; and Tang, Y. 1998. Paleozoic tectonic evolution of the Tianshan Orogen, northwestern China. Tectonophysics 287:213–231.

Gao, J.; Zhang, L.; and Liu, S. 2000. The $^{40}Ar/^{39}Ar$ age record of formation and uplift of the blueschists and eclogites in the western Tianshan Mountains. Chin. Sci. Bull. 45:1047–1051.

Harrison, T. M., and McDougall, I. 1980. Investigations of an intrusive contact, northwest Nelson, New Zealand. II. Diffusion of radiogenic and excess ^{40}Ar in hornblende revealed by $^{40}Ar/^{39}Ar$ age spectrum analysis. Geochim. Cosmochim. Acta 44:2005–2020.

Hodges, K. V. 1991. Pressure-temperature-time paths. Annu. Rev. Earth Planet. Sci. 19:207–236.

Klemd, R. 2003. Ultrahigh-pressure metamorphism in eclogites from the western Tianshan high-pressure belt (Xinjiang western China): comment. Am. Mineral. 88:1153–1156.

Klemd, R.; Schröter, F.; Will, T. M.; and Gao, J. 2002. PT-evolution of glaucophane-clinozoisite bearing HP-LT rocks in the western Tianshan orogen, NW China. J. Metamorph. Geol. 20:239–254.

Kretz, R. 1983. Symbols for rock-forming minerals. Am. Mineral. 68:277–279.

Scaillet, S. 1998. K-Ar ($^{40}Ar/^{39}Ar$) geochronology of ultrahigh pressure rocks. *In* Hacker, B. R., and Liou, J. G., eds. When continents collide: geodynamics and geochemistry of ultrahigh-pressure rocks. Dordrecht, Kluwer Academic, p. 161–201.

Sherlock, S. C., and Arnaud, N. 1999. Flat plateau and impossible isochrons: apparent ^{40}Ar-^{39}Ar geochronology in a high-pressure terrain. Geochim. Cosmochim. Acta 63:2835–2838.

Sherlock, S. C., and Kelley, S. 2002. Excess argon evolution in HP-LT rocks: a UVLAMP study of phengite and K-free minerals, NW Turkey. Chem. Geol. 182: 619–636.

Sobolev, N. V.; Dobretsov, N. L.; Bakirov, L. B.; and Shatsky, V. S. 1986. Eclogites from various types of metamorphic complexes in the USSR and the problems of their origin. *In* Evans, B. W., and Brown, E. H., eds. Blueschists and eclogites. Geol. Soc. Am. Mem. 164: 349–363.

Tagiri, M.; Yano, T.; Bakirov, A.; Nakajima, T.; and Uchiumi, S. 1995. Mineral parageneses and metamorphic P-T paths of ultrahigh-pressure eclogites from Kyrghyzstan Tien-Shan. Island Arc 4:280–292.

Volkova, N. I., and Budanov, V. I. 1999. Geochemical

discrimination of metabasalt rocks of the Fan-Karategin transitional blueschist/greenschist belt, South Tianshan, Tajikistan: seamount volcanism and accretionary tectonics. Lithos 47:210–216.

Wei, C. J.; Powell, R.; and Zhang, L. F. 2003. Eclogites from the south Tianshan, NW China: petrological characteristic and calculated mineral equilibria in the Na_2O-CaO-FeO-MgO-Al_2O_3-SiO_2-H_2O system. J. Metamorph. Geol. 21:169–179.

Wemmer, K. 1991. K/Ar-Alterdatierungsmöglichkeiten für retrograde Deformationsprozesse im spröden und duktilen Bereich: Beispiele aus der KTB-Vorbohrung (Oberpfalz) und dem Bereich der Insubrischen Linie (N-Italien). Göttinger Arb. Geol. Paleontol. 51:1–61.

Xiao, X. C.; Tang, Y. Q.; and Feng, Y. M. 1992. Tectonics of North Xinjiang and its adjacent region. Beijing, Geological Publishing House, p. 55–60. (In Chinese.)

Zhang, L.; Ellis, D. J.; Arculus, R. J.; Jiang, W.; and Wie, C. 2003*a*. "Forbidden zone" subduction of sediments to 159 km depth: the reaction of dolomite to magnesite + aragonite in the UHPM metapelites from western Tianshan. China. J. Metamorph. Geol. 21: 523–529.

Zhang, L.; Ellis, D. J.; and Jiang, W. 2002*a*. UHP metamorphism in western Tianshan, China. I. Evidences from coesite pseudomorphs in garnet and quartz exsolution in omphacite and in eclogites. Am. Mineral. 87:853–860.

Zhang, L.; Ellis, D. J.; Jiang, W.; Wei, C.; and Ye, J. 2002*b*. UHP magnesite-bearing metapelites from west Tianshan, China: P-T-X_{CO2} paths and SHRIMP dating. Proceedings for Intern. UHPM-workshop, September 20–21, 2002, Beijing, p. 77.

Zhang, L.; Ellis, D. J.; Williams, S.; and Jiang, W. 2003*b*. Ultrahigh-pressure metamorphism in eclogites from the western Tianshan high-pressure belt (Xinjiang western China): reply. Am. Mineral. 88:1157–1160.